An Ultra Low Power CMOS pA/V Transconductor and its Application to Wavelet Filters

Peterson R. Agostinho[1, 2], Sandro Haddad[2,3], Jader A. De Lima[3]
Wouter A. Serdijn[2] and Osamu Saotome[1]

1. Technological Institute of Aeronautics, Electrical Eng. Dept, São José dos Campos - SP, Brazil
2. Electronics Research Laboratory, Faculty of Electrical Eng., Delft University of Technology, Delft, The Netherlands
3. Brazil Semiconductor Technology Center, Freescale Semiconductor, 13820-000 Jaguariúna – SP, Brazil

ABSTRACT
Two topologies of ultra low-power CMOS triode transconductor are proposed. Its input transistors are kept in the triode region to benefit from the lowest g_m/I_D ratio. The g_m is adjusted by a well defined (W/L) and V_{DS}, the latter a replica of the tuning voltage V_{TUNE}. Transconductance down to hundreds of pA/V are obtained and used to implement a 6th order wavelet filter. The resulting design complies with a 1.5V supply and a 0.35µm CMOS process. The total power consumption of the wavelet filters using the first and second topology of transconductor equals 51nW and 114nW, respectively.

Categories and Subject Descriptors
B.7.1 [**Integrated Circuits**]: Types and Design Styles - *Advanced technologies, VLSI (very large scale integration).*

General Terms
Performance, Design, Standardization.

Keywords
Low-power, pa/V, transconductor.

1. INTRODUCTION
In the field of medical electronics, active filters with large time constants are often required to design low cutoff-frequency filters (in the Hz and sub-Hz range), demanding the use of large capacitors or very low transconductance. To limit capacitors to practicable values, a transconductor with an extremely small transconductance g_m is needed.

This paper presents two topologies of ultra low-power transconductor. Both configurations are compact and have their input transistors operating in the triode region to benefit from the lowest g_m/I_D ratio and linear variation of g_m, which is controlled by an external voltage V_{TUNE}. The advantages of this technique with respect to the techniques that employ voltage attenuation, source degeneration or current splitting [2-5] can be found in [1].

The first g_m, named VLPT-g_m (very low-power triode g_m), with transconductance in the range of few nA/V. The second configuration, named Delta-g_m, is presented here and the g_m can be adjusted to values down to hundreds of pA/V.

Subsequently, this paper presents an implementation of the wavelet transform with a Gaussian wavelet (*gaus1*) in an ultra low-power environment, using the proposed transconductors. Low-power analog realization of the continuous wavelet transform enables its application *in vivo*, e.g. in pacemakers and IECG recorders.

Previous work on analog realization of the continuous wavelet transform uses the dynamic-translinear circuit technique [6]. Contrary to this approach, the g_m is now controlled by voltage rather than by current. Translinear circuits become difficult to integrate when designing low cutoff-frequency filters for use in the Hz and sub-Hz range. As an example, for g_m = 1nA/V, the VLPT-g_m needs to be biased with a quiescent current around I_Q = 300pA. To achieve the same time constant and considering the same bias current, the translinear circuit needs an increase of 12.6 times in capacitor value. Or, to maintain the same capacitor, it is necessary to decrease the current to 25pA, which is difficult to obtain precisely.

Since (W/L) offers a degree of freedom in sizing g_m, V_{DS} values well above the equivalent noise of the biasing circuit can be set, while still obtaining a very-low g_m. Consequently, filters with more predictable frequency characteristics can be implemented. Owing to its extended linearity, the triode-MOSFET transconductor also handles larger signals, with no need for linearization techniques.

The paper organization is as follows. Section 2 introduces the triode transconductors circuits. Design procedures for realizing appropriate g_m values and implementing the wavelet filter are discussed in Section 3. Simulation results are used to demonstrate circuit performance and tunability in Section 4. Conclusions and final remarks are given in Section 5.

2. TRANSCONDUCTORS DESCRIPTION
The proposed triode transconductors are shown in Fig. 1. Fig.1a shows the VLPT-gm, that is an improvement of the circuit introduced in [1]. The main difference of these circuits is the introduction of a common-gate stage M_{3A}-M_{3B} into the loop of the auxiliary amplifier. The transconductor equivalent noise and output swing remain practically the same. However there is a great improvement in the auxiliary amplifier loop gain and transconductor output resistance R_{OUT}, as shown in Fig. 2.

Here, A_{L1} and A_{L2} represent the loop gain of the auxiliary amplifier in the original circuit in [1] and in the proposed transconductor, respectively, and are given by

$$A_{L1} \cong g_{m2} r_{ds2}, A_{L2} \cong g_{m2} r_{ds2} g_{m3} r_{ds3} \quad (1)$$

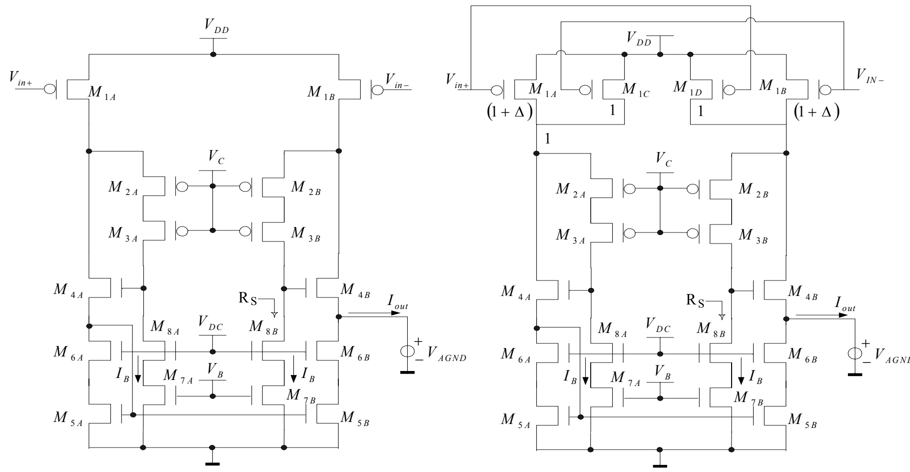

(a) (b)

Fig. 1.Triode Transconductors a)VLPT-g_m and b) Delta-g_m

Input transistors M_{1A}-M_{1B} have their drain voltages regulated by an auxiliary amplifier that comprises M_{2A}-M_{2B}, M_{3A}-M_{3B}, M_{4A}-M_{4B} and bias current sources M_{7A}-M_{7B} and M_{8A}-M_{8B}. Internal voltages V_B, V_C and V_{DC} are derived from the bias circuit shown in Fig.3.

The bias generator is structurally alike the transconductor so that the external voltage V_{TUNE} is reflected to the drain of M_{1A}-M_{1B}. A low voltage cascade current mirror comprising M_{5A}-M_{5B} and M_{6A}-M_{6B} provides a single-ended output.

Even though a common-drain configuration M_4 is seen from the output node, the transconductor still exhibits a high output resistance, as the loop gain around M_2, M_3 and M_4 is very large. Current sources M_7 and M_8 biased in their weak inversion region provide an output resistance, seen from the drain terminal of M_8, R_S, in the order of $10^{11}\Omega$, so that an output resistance R_{OUT} of the same order is obtained.

The gate-voltage of M_{2A}-M_{2B} is set to V_C=V_{TUNE}–V_{GS2}, whereas V_B imposes a bias current I_B through M_{7A}-M_{7B}. Both voltages V_B and V_C are on-chip generated. Referring V_{TUNE} to V_{DD} and denoting β_1=$(W/L)1\mu_pC_{ox}$, the transconductance of the entire circuit is

$$g_m = g_{m1} = \beta_1 V_{TUNE} \qquad (2)$$

A second transconductor Delta-gm is shown in Fig.1b. The aspect-ratios of input transistors (M_{1A}-M_{1D}) are $(W/L)_{A,B} = (1+\Delta)(W/L)_{C,D}$.

Considering a balanced small signal voltage applied in V_{in+} and V_{in-} the output current is given by

$$\begin{aligned} i_{OUT} &= (i_{1B} + i_{1D}) - (i_{1A} + i_{1C}) \\ i_{OUT} &= \frac{v_{IN}}{2} g_{m1D}\Delta + \frac{v_{IN}}{2} g_{m1C} \\ \therefore i_{OUT} &= \Delta g_{m1C,D} v_{IN} \end{aligned} \qquad (3)$$

Referring V_{TUNE} to V_{DD} and denoting β=$(W/L)\mu_pC_{ox}$, the overall transconductance is

$$g_m = \Delta g_{m1C,D} = \Delta\beta_{1C,D} V_{TUNE} \qquad (4)$$

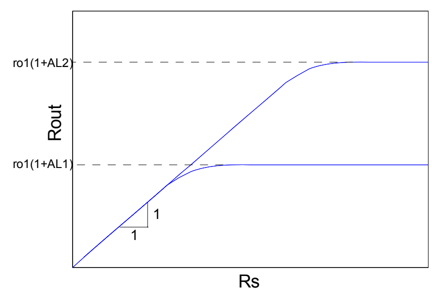

Fig. 2. Transconductor introduced in [1] and proposed transconductor output resistance as function of R_S

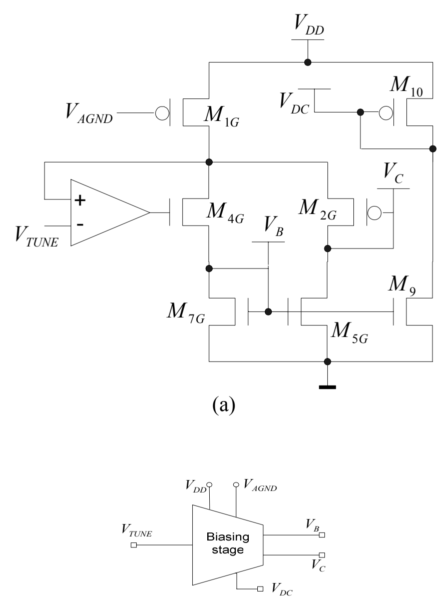

(b)

Fig. 3. Bias generator [1]: (a) circuit diagram and (b) the corresponding symbol

3. WAVELET FILTER DESIGN

3.A. L_2 approximation

As mentioned in [6], approximation methods should be applied to obtain the required transfer function of a wavelet filter's impulse response. A method which proves to be successful is provided by Padé approximation of the Laplace transform of the impulse response h(t) of the filter [6]. Another alternative to find a suitable wavelet base approximation can be provided by the theory of L_2 approximation [7].

The advantage of the L_2 method compared to the Padé approximation is that the L_2 approximation offers a more global approximation, i.e., not concentrating on one particular point --- Padé is usually computed at the origin. Also, the fit is performed directly in the time domain yielding good control and easy interpretation of the optimization criteria. The L_2 approximation technique is based on minimizing the least-mean-square-error. In this scheme the error integral, which is the difference between the wavelet function $\psi(t)$ and its approximation h(t), is defined by

$$\varepsilon_{L2} = \int_0^\infty \left(\psi(t) - h(t)\right)^2 dt \qquad (5)$$

In this L_2 approach we first express the impulse response (in time domain) of a general filter. After that, the error ε_{L2} is minimized with respect to the poles and zeros of the wavelet filter. For the generic situation of stable systems with distinct poles, h(t) may typically have the following form [7]

$$h(t) = \sum_{i=1}^{n} A_i e^{P_i t} = \sum_{i=1}^{k} c_i e^{p_i t} + c_{k+1} e^{p_{k+1} t} \sin(p_{k+2} t) + \qquad (6)$$
$$c_{k+2} e^{p_{k+1} t} \cos(p_{k+2} t) + \cdots + c_{n-1} e^{p_{n-1} t} \sin(p_n t) + c_n e^{p_{n-1} t} \cos(p_n t)$$

where A_i and P_i can be real or complex numbers; c_i and p_i are real numbers, representing the impulse response function h(t) as a linear combination of damped exponentials and exponentially damped harmonics. *k* corresponds to the number of real poles and *n* is the order of the filter.

Then, given the explicit form of a wavelet base $\psi(t)$ and the approximated impulse response h(t), the L_2-norm of the difference $\psi(t)$-h(t) can now minimized in a straightforward way using standard numerical optimization techniques and software. The most direct way to find the minimum of Eq.5 is by computation of all partial derivatives of ε_{L2} with respect to A_i and P_i and setting them equal to zero, namely

$$\frac{\partial \varepsilon_{L2}}{\partial A_i}, \frac{\partial \varepsilon_{L2}}{\partial P_i} = 0 \qquad for \qquad i = 1 \ldots n \qquad (7)$$

The wavelet base approximation using the proposed L_2 approach is given in Fig.4, where the first derivative of a Gaussian wavelet base (*gaus1*) has been approximated using the corresponding 6^{th}-order transfer function

$$H(s) = \frac{0.16s^4 - 8.32s^3 + 6.64s^2 - 139s}{s^6 + 5.9s^5 + 30.5s^4 + 83.1s^3 + 163s^2 + 176s + 93.3} \qquad (8)$$

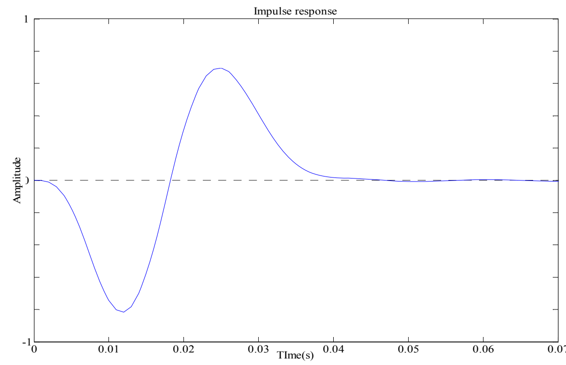

Fig. 4. L_2 approximation of the first derivative of Gaussian

3.B. State-space filter implementation

To meet low-power low-voltage requirements, the state-space description of the filter has been optimized with respect to dynamic range, sparsity and sensitivity [6]. The filter design that follows is based on an orthonormal ladder structure and employs the nano-power g_m transconductor described in the previous section as the basic building block of the filter diagram in Fig.5. In order to obtain the corresponding gm-C filter realization, we need first to map the state-space coefficients on the respective g_m values. From Eq.2 of the transconductance, one can notice that we may vary the value of g_m by changing β_1 (the aspect ration W/L) or the drain-source voltage (V_{TUNE}) of transistor M1. However, due to the additional bias stages required to obtain different filter coefficients, realization of the various V_{TUNE} bias generators would increase the power consumption by a factor of $(n-1)\cdot P_{Bias}$, where *n* is the number of implemented coefficients and P_{Bias} represents the power consumption of the biasing stage. We thus opt for changing g_m by changing β_1.

4. SIMULATION RESULTS

To validate the circuit principle, we have simulated the wavelet Gm-C filter using models of AMS's 0.35µm CMOS IC technology. The circuit has been designed to operate from a 1.5-V supply voltage. In order to implement the different coefficients of the state-space representation we can vary the width of input transistors M_1 or the value of V_{TUNE}.

Fig. 5 shows the block diagram of the wavelet filter and the value of each g_m, which were reached by varying the width of input transistors @V_{TUNE}=20mV. In Fig.6 one can see g_m ranging from 1nA/V to 5nA/V by changing V_{TUNE} from 10mV to 50mV.

Finally, to implement a Wavelet Transform, we need to be able to scale and shift in time (and, consequently in frequency) the *gaus1* function. By changing the values of the V_{TUNE} accordingly we implement different scales, while preserving the impulse response waveform, as one can see in Fig.7.

Fig.8b illustrates 4 dyadic scales with center frequencies ranging from 14Hz to 120Hz for V_{TUNE} varying from 10mV to 80mV, respectively

Fig.9 shows the total harmonic distortion (THD) of VLPT-g_m and Delta-g_m with respect do V_{TUNE}. One can see a distortion THD < -46dB for the range10mV < V_{TUNE} < 80mV.

	VLPT - gm	Delta - gm
gm1 [nA/V]	1,18	0,47
gm2 [nA/V]	1,64	0,66
gm3 [nA/V]	2,00	0,80
gm4 [nA/V]	2,43	0,97
gm5 [nA/V]	4,06	1,62
gm6 [nA/V]	5,93	2,37
gm7 [nA/V]	1,30	0,52
gm8 [nA/V]	1,00	0,40
gm9 [nA/V]	2,00	4,80
gm10 [nA/V]	1,20	0,48
C [pF]	6 x 20	6 x 8

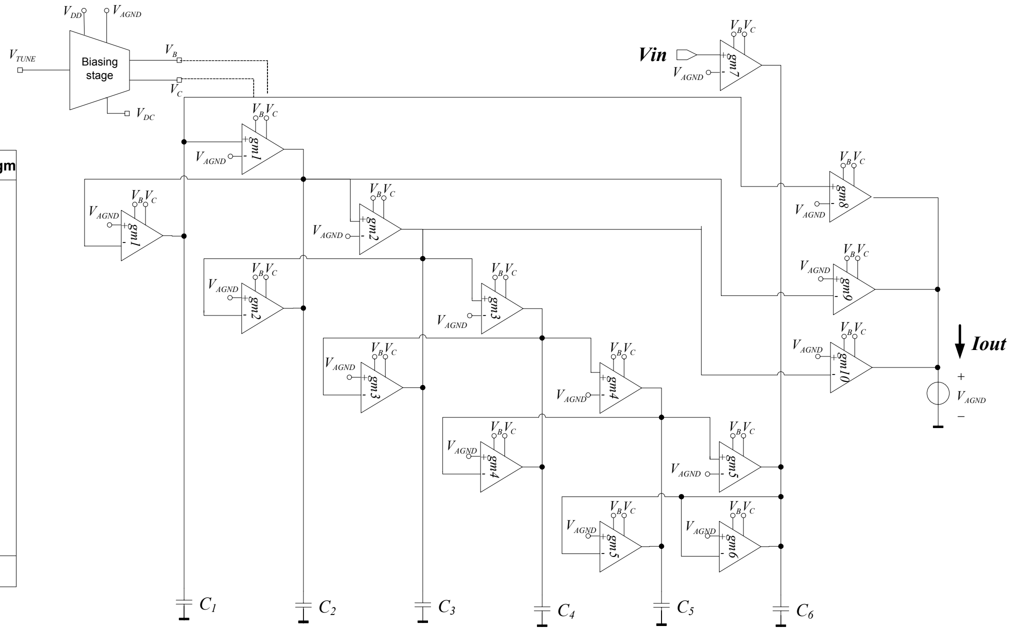

Fig. 5. Block diagram of the wavelet filter

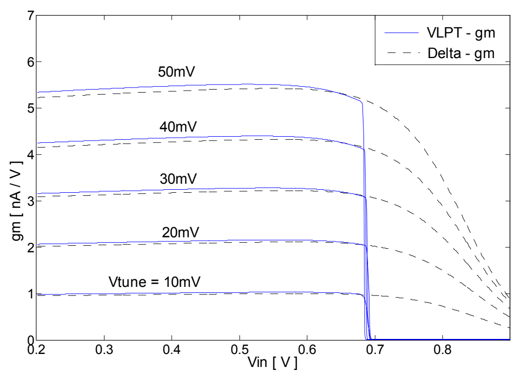

Fig. 6. Different g_m values obtained by varying V_{TUNE}

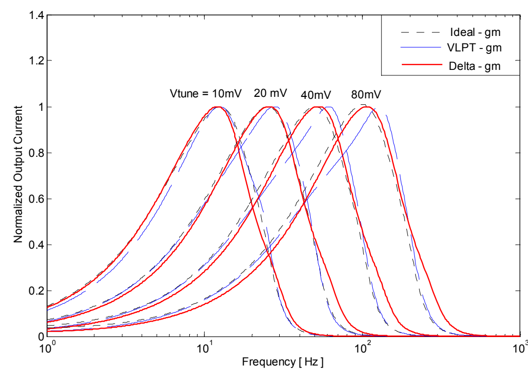

Fig. 8 Frequency response filter scaling by changing V_{TUNE}

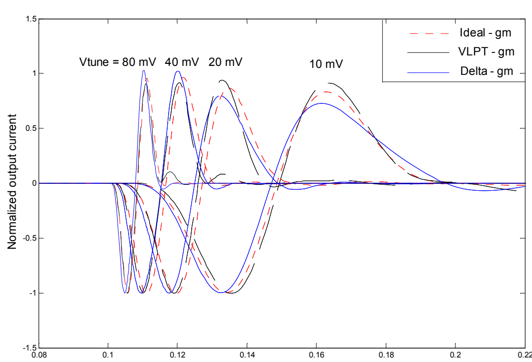

Fig. 7 Impulse response filter scaling by changing V_{TUNE}

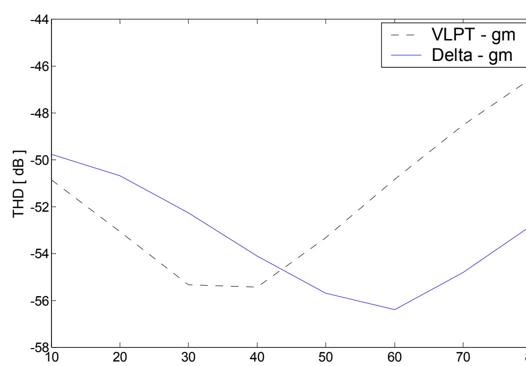

Fig. 9. THD values obtained by varying V_{TUNE}

Monte Carlo analysis for a spread of 5% on both (W/L) and V_{T0} parameters on input transistors of the g_m revealed a maximum variation of 2.6% in the transconductance value of VLPT-g_m. Fig. 10 shows, for the same Monte Carlo analysis, the g_m variation of Delta-g_m by changing the value of Delta.

A transconductor with Delta = 0.4 was set to implement the wavelet filter. One can thus see the trade-off between the value of g_m and precision of the transconductance.

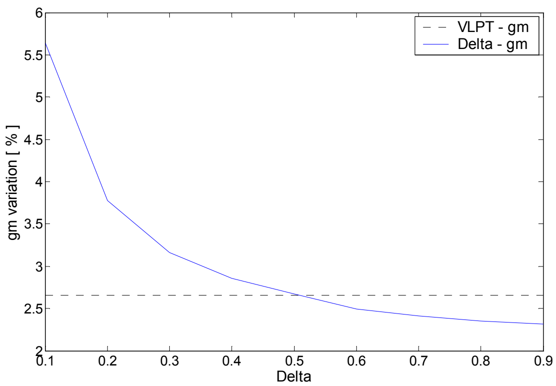

Fig. 10. g_m variation in Monte Carlo analysis by changing delta

Table 1 shows the summary of the simulated results. The total power consumption of Delta-g_m filter equals 114nW, a factor of two compared with Delta-g_m. Input-referred noise is 156µV/√Hz @1Hz and 119µV/√Hz @100Hz for VLPT-g_m. Output resistance and distortion have similar results for both topologies. The great advantage of Delta-g_m is its minimum value of transconductance and greater bandwidth. For example, with delta = 0.15 (g_m variation around 5%), a minimum transconductance of 150pA/V is achieved. And for Delta = 0.4 the 3dB frequency of 1nA/V is 1.33 kHz and 24 kHz for VLPT-gm and Delta-gm, respectively. Such an improvement in the frequency response is due to the reduction of the dimension of transistors in the implementation of Delta-g_m.

Table 1 – Summary of simulated results

	VLPT-gm	Delta-gm
Filter Power [nW]	51n	114
g_m Band-width [kHz], delta=0.4	1.33	24
Input Eq. Noise @ 1Hz	156	642
Input Eq. Noise @ 100Hz	119	460
Minimum g_m [nA/V]	≅ 1	≅ 0.15
Rout @g_m = 2nA/V [Ω]	1×10^{11}	4×10^{10}
gm variation[%],delta = 0.4	2.7	2.9
g_m variation[%],delta = 0.15	2.7	5
THD[dB], V_{TUNE} = 20mV	-53	-51
THD[dB], V_{TUNE} = 80mV	-47	-53

5. CONCLUSION

Two compact CMOS transconductors suitable for ultra-low power gm-C filters operating in the Hz and sub-Hz range have been proposed. Its input transistors are kept in the triode-region to benefit from the lowest g_m/I_D ratio. To validate the circuit principle, the transconductors were used to implement a wavelet transform with a Gaussian wavelet using a 6th order L_2 approximation.

The design was realized in accordance with VDD=1.5V and a 0.35µm n-well CMOS process. Simulation data were obtained with PSPICE and Bsim3v3 models. For the VLPT-g_m, the transconductance ranges from 1nA/V to 12nA/V, total power consumption equals 51nW, for a total capacitance of 120pF. For Delta-gm filter, g_m spans from 400pA/V to 4.8nA/V, with total power consumption of 114nW, for a total capacitance of 48pF. THD < 1% @200mVpeak_value was reached for every transconductor of the filters.

The simulated step response of 6th order wavelet filter differs only slightly from the approximated response in both topologies. From this, we can conclude that the coefficients have been implemented successfully.

6. ACKNOWLEDGEMENTS

The authors would like to thank Joel M.H. Karel, Ralf L.M. Peeters and Ronald L. Westra from Department of Mathematics, University of Maastricht, The Netherlands for their mathematical assistance and the University Program ITA-SAT for the financial support.

7. REFERENCES

[1] J.A. de Lima and W.A. Serdijn - "Compact nA/V Triode-MOSFET Transconductor", Electronics Letters, Vol. 41, pp. 1113-1114, 2005.

[2] Veeravalli, A. et al.–"Transconductance Amplifier Structures With Very Small Transconductances: A Comparative Design Approach", IEEE JSSC, Vol. 37, No. 6, pp 770-775, June 2002

[3] Silva-Martínez, J. & Salcedo-Suner – "IC Voltage to Current Transducers with Very Small Transconductances", Analog Int. Circuits and Signal Processing, Vol. 13, pp 285-293, 1997

[4] Steyaert, M., Kinget, P., Sansen, W. & Van Der Spigel, J. – "Full Integration of Extremely Large Time Constants in CMOS", Electronics Letters, Vol. 27, No. 10, pp. 790-791, 1991

[5] Arnaud, A. & Galup-Montoro, C. – "A Fully Integrated 0.5-7 Hz CMOS Bandpass Amplifier", Proc. of IEEE ISCAS, Vol. 1, pp. 445 – 448, Vancouver, Canada, 2004

[6] S.A.P. Haddad, S. Bagga and W.A. Serdijn, "Log-domain wavelet bases," *IEEE Transactions on Circuits and Systems – I: Regular Papers*, vol. 52, no. 10, Oct. 2005

[7] J.M.H. Karel, R.L.M. Peeters, R.L. Westra, S.A.P. Haddad, W.A. Serdijn, "Wavelet approximation for implementation in dynamic translinear circuits", proc. *IFAC World Congress 2005*, Prague, July 4-8, 2005